

A STUDY OF COSMIC RADIATION
USING A LARGE CRYSTAL TOTAL ABSORPTION SPECTROMETER

A Thesis

Submitted to

Faculty of Graduate Studies, University
of Manitoba, in partial fulfillment of
the requirements of the Degree of Master
of Science.



By

Fook-Kit Chin

Winnipeg, Manitoba

August, 1961

ACKNOWLEDGEMENTS

The writer wishes to express his gratitude to Dr. S. Standil, the director, for his continuing guidance and valuable suggestions during the time of this research and the preparation of this thesis.

Sincere thanks are due to Mr. R.P. Bukata for his help in doing the experiments, to Mr. R.S. Foulds for his technical assistance in maintaining the electronics, and to Mr. P.S. Lindsay for his constructing the steel-bar frame used in the lead absorption experiment.

Acknowledgements are also gratefully made to the Research Corporation and the National Research Council of Canada for the financial support to this research, and to the Department of Transport, Winnipeg for the supply of daily weather reports.

A B S T R A C T

A large NaI (Tl) crystal total absorption spectrometer was used for the following studies on the cosmic radiation near sea level: (a) the differential energy loss spectra of the total radiation and of the neutral component, (b) day-night variations of the intensity of the total radiation and of the neutral component, and (c) a sudden increase in the photon component on May 4, 1960.

Observed energy spectra are presented and discussed. No statistically significant day-night effect was established. The sudden increase in the photon component was found to be related to a solar flare occurring about 25 minutes earlier.

C O N T E N T S

Acknowledgements	i
Abstract	ii
Contents	iii
Chapter I. Introduction	1
Chapter II. Experimental Techniques	3
A. The Total Absorption Spectrometer and the Recording Electronics	3
B. Characteristics of the Whole Apparatus in Detecting Cosmic Rays	5
(i) Without Anticoincidence Shield	5
(ii) With Anticoincidence Shield	6
a. Interaction between Neutral Particles and Matter	6
b. Function as Total Absorption Spectrometer for Neutral Component	10
c. The Response of the Spectrometer to Neutral Particles	11
d. Efficiency of Shield in Eliminating Charged Component	13
C. Determination of the Differential Spectrum	14
Chapter III. Experimental Results	16
A. Energy Spectra	17
(i) Differential Energy Spectra	17
(ii) Relative Intensities of the Neutral to the Total Radiation	19
a. Ratio of Detected Neutral to Detected Total Radiation	19
b. Ratio of Totally Absorbed Neutral to Totally Absorbed Cosmic Radiation	20

(iii) Comparison of Energy Spectra Observed in 1960 and 1961	21
B. Nature of the Neutral Component as Detected by the Spectrometer	22
C. Day-Night Variation of Cosmic Radiation	27
(i) The Mu-Peak Region	27
(ii) Neutral Component	28
D. A Sudden Increase in the Photon Component of Cosmic Radiation	32
E. Conclusions	33
References	34
Diagrams	36

CHAPTER I
INTRODUCTION

The nature and intensity of cosmic radiation near sea level has been studied for more than two decades, yet reports on the sea level photon component alone are meager. This is primarily due to the late development of suitable detectors for such studies.

Previous work on the high energy cosmic photons usually make use of the fact that the soft component (electrons and photons) generates showers of secondary particles in dense matter. By the coincidence method using counter arrays, the nonionizing particle which produces a shower in a dense absorber is a photon. Through the shower theory, the number of shower particles is related to the energy of the primary photon. Thus, the energy spectrum of photons near sea level has been determined by Janossy and Rossi (1940), Clay and van Alphen (1951), Chou (1953), Cernigoi and Poiani (1954), and Kameda (1960); their results are consistent in that the differential energy distribution obeys a power law but differ in the values of the exponent from -2.1 to -2.8 for the energy range around 1 Bev. No information has been reported for similar studies in the low energy region i.e. up to a few hundred Mev. This thesis presents preliminary results, using a newly developed instrument, of such a study.

The introduction of the scintillation method in 1944 and the later development of large scintillation phosphors and associated counter equipment made high energy photon studies possible. However,

a simple and effective separation of the photon component from the total cosmic radiation still remained as a challenging problem. At the University of Manitoba, a large NaI (Tl) crystal total absorption spectrometer was designed by Standil and Loveridge (1959) primarily for the study of the photon component and it has been used for a time variation study of the neutral component of the cosmic radiation (see Bukata, 1960). In this thesis, the main characteristics of this spectrometer were discussed, the general features and the time variation of the differential spectrum obtained with this spectrometer were studied, and day-night effects on the cosmic radiation were investigated in a preliminary way.

CHAPTER II

EXPERIMENTAL TECHNIQUES

Experiments were done in the Cosmic Ray Laboratory of the University of Manitoba which is located on the roof of the old Science Building, geographic latitude 49.9° N, longitude 97.2° W, and an elevation of 236 meters above sea level. The walls of the laboratory were made of wood, and the construction material of the roof was chosen such that the effects due to the transition of cosmic rays through matter would be minimized. The instability of the electronics resulting from the temperature change was eliminated by means of an air conditioning system which kept the room temperature at $70 \pm 2^{\circ}$ F all the time. Studies on high energy cosmic radiation were carried out with a large NaI (Tl) crystal total absorption spectrometer as the detector and a conventional arrangement of electronics as the events recorder, and data were collected in terms of differential energy loss spectra.

A. The Total Absorption Spectrometer and the Recording Electronics

It has been established that the cosmic radiation inside the atmosphere is composed of charged and neutral particles. The present total absorption spectrometer was primarily designed to separate the neutral component from the total radiation. Functionally speaking, the whole experimental arrangement consists of two systems; namely, the signal system which produces signal pulses upon detecting charged or uncharged particles, and the anticoincidence system which provides anticoincidence pulses for the cancellation of the charged or not totally absorbed particles; and a final recorder which presents a differential spectrum

for the total radiation if it receives signal pulses from the system of signal alone, and a spectrum for the neutral component if both systems are operated simultaneously. Detailed information about the total absorption spectrometer and the recording electronics can be found in the reports of Standil (1959), Loveridge (1959), and Bukata (1958, 1959) while a simple description is given here for the convenience of reading this thesis.

The signal system contains a NaI (thallium activated) crystal with a cylindrical shape of $9\text{-}\frac{3}{8}$ inches in diameter, $8\text{-}\frac{11}{16}$ inches in height and a 45° bevel to a cone of $2\text{-}\frac{5}{8}$ inches in diameter as shown in Figure 1. When a cosmic ray particle, either charged or neutral, interacts with the crystal a flash of light is generated, the quantity of which is proportional to the amount of energy lost by the impinging particle in the crystal. Three photomultipliers that view the bottom plane face of the crystal through a glass light pipe will pick up and convert the emitted light into electrical pulses which are electronically summed up with a three channel mixer into a pulse designated as signal pulse. Being small in size, this pulse is further magnified by means of a linear amplifier before it is sorted into the proper channel of a hundred channel kicksorter (see Figure 2).

As for the anticoincidence system, a cylindrical shield of plastic phosphor (type NE 102) was constructed to envelope the NaI crystal entirely by means of four sections: a circular top plate of 26 inches in diameter and 1 inch in thickness, two identical sections of hollow cylinder with an outer diameter of 26 inches and an inner diameter of 16 inches and a height of $11\text{-}\frac{1}{2}$ inches, and a cylindrical bottom of 26 inches in diameter and 6 inches in thickness. Six photomultipliers were installed around the edge of the top plate, and five were placed directly under the

bottom section. These eleven photomultipliers collect the light emitted in the anticoincidence shield due to the interaction between the cosmic radiation and the plastic phosphor, and convert it into electrical pulses which are added together in an eleven channel mixer as a pulse called the a. c. pulse. Having been amplified by a linear amplifier, this a. c. pulse, if its size is above the bias setting of the gate pulse generator, will trigger the generator to produce a negative output pulse of constant size about 50 volts and 4 microseconds which is fed into the anticoincidence input circuit of the hundred channel kicksorter.

As a result, events in the signal system unaccompanied by events in the anticoincidence system are ascribed to the neutral particles which are totally absorbed by the crystal, while charged and neutral events are recorded if the anticoincidence system is absent in the operation. The total absorption spectrometer which consists of the NaI crystal and the shield, and the block diagram of the whole experimental arrangement are shown in Figure 1 and Figure 2.

B. Characteristics of the Whole Apparatus in Detecting Cosmic Rays

To clarify the foregoing description, let us discuss the characteristics of the instrument operated without the anticoincidence shield and of the instrument operated with the anticoincidence shield.

(i) Without Anticoincidence Shield

The NaI crystal, by itself alone, can detect charged and uncharged cosmic particles coming from all directions, and the differential energy spectrum thus obtained gives the energy loss distribution for the total radiation in the crystal. This differential spectrum is not an energy spectrum in an absolute sense because the energy loss in the crystal does not necessarily identify the entire energy possessed by the

particle detected. For instance, when a charged particle hits the crystal, it gives up part of its energy as ionization loss in the plastic phosphor shield, and it may pass through the NaI crystal after transferring another part of its energy to the crystal; therefore, the energy recorded by the apparatus is not the total energy of this particle. However, if the particle is totally absorbed by the crystal the energy recorded is the total energy possessed by the particle when it entered the crystal.

(ii) With Anticoincidence Shield

The characteristics of the combined operation of the signal and the anticoincidence systems can be discussed in three aspects; namely, its service as a total absorption spectrometer for the neutral component, its response to different kinds of neutral particles, and its efficiency in eliminating the charged component. To begin with, let us survey the properties of the interactions between the cosmic neutral particles and the matter which constitutes the detectors.

a. Interaction between Neutral Particles and Matter

Since almost all of the neutral particles near sea level are photons and neutrons, only these need be considered. Being electrically uncharged, neither photons nor neutrons suffer from any ionization loss during their passage through matter. Incident upon matter, a photon will either pass through without any loss in its energy, or interact through the photoelectric effect, Compton scattering, or pair production with a definite probability for each process. Also, if the mean free path of the primary photon is much less than the thickness of the absorber there is a high probability for the total absorption of the resulting secondary particles such as electron pairs, bremsstrahlung, X-rays etc. The same is generally true for the interaction between neutrons and matter except that nuclear interaction processes such as (n, gamma),

(n, n), and (n, ionizing particles) take place first. The probability of interaction (P) between a neutral particle with a certain energy and the absorber as well as its mean free path (m.f.p.) in the absorber are estimated through the following standard formulas:

$$P = 1 - e^{-Tt}$$

$$\text{m.f.p.} = 1/T$$

where T is the linear absorption coefficient of the absorber for a particular incident particle with a specified energy and t is the distance traversed by the particle concerned.

The geometric dimensions of the present NaI crystal are shown in Figure 1. Taking its density value as 3.67 gm/c.c. (Harshaw, 1960) and assuming an averaged traversed distance as about 7 inches (or about 17.8 cm), the probabilities of interaction between the crystal and photons of different energy values as well as the corresponding mean free paths are calculated in Table 1. ($T_{\text{NaI, photon}}$ = mass absorption coefficient of NaI for photon \times density of NaI, the mass absorption coefficients being obtained from Siegbahn's book (1955)).

Table 1

<u>Photon Energy</u> (Mev)	<u>Mass Absorption Coeff. of NaI</u> (cm ² /gm)	<u>Mean Free Path</u> (cm)	<u>Probability of Interaction in NaI</u>
10	0.0329	8.3	0.884
20	0.0419	6.5	0.936
30	0.0472	5.8	0.955
40	0.0511	5.3	0.964
50	0.0544	5.0	0.972
60	0.0571	4.8	0.976
80	0.0601	4.5	0.980
100	0.0630	4.3	0.984

As for the interaction between the NaI and neutrons, only a rough estimation can be made, partly because the available data of neutron

total cross sections for Na and I with energy greater than 10 Mev are scarce and partly because they include the (n, n) process whose partial cross section has not been well established. Since the NaI crystal emits light only when it interacts with ionizing particles, allowance must be made for the contribution of the (n, n) process when we estimate the probability of interaction between neutrons and the crystal which is at present assumed to be equal to the probability of detection. From the neutron cross section data edited by Hughes and Schwartz (1958), the neutron total cross sections for Na (S_{Na}) and for I (S_I) seem to be constant for energy greater than 10 Mev, and their values are 2 barns and 4 barns respectively. To ascertain the contribution of the (n, n) process, we take half of the total cross section as due to the elastic neutron scattering for both cases of Na and I by referring to the data for Mg (neighbouring element to Na) and Sn (neighbouring element to I). Therefore, the effective total cross section of NaI ($S_{NaI, \text{neutron}}$) is taken as one half of the sum of S_{Na} and S_I . With

$$T_{NaI, \text{neutron}} = S_{NaI, \text{neutron}} \times N_{NaI}$$

and

$$N = \frac{\text{Avagadro's Number} \times \text{Density of NaI}}{\text{Molecular Weight of NaI}}$$

(N is the number of molecules in 1 c.c. of NaI)

Avagadro's Number = 6.02×10^{23} / gram mole

Molecular Weight of NaI = 149.92 gm

(values are obtained from the standard handbook for physics and chemistry)

the result is given in Table 2.

Table 2

<u>Neutron Energy</u> (Mev)	<u>Total Cross Sections</u>		<u>Mean Free Path</u> (cm)	<u>Probability of Interaction in NaI</u>
	S_{Na} ($\times 10^{24}$ cm ²)	S_I ($\times 10^{24}$ cm ²)		
E > 10	2.0	4.0	22.6	0.545

The properties of the plastic phosphor and the formula of the mass absorption coefficient of the plastic phosphor for photons (U_{ph}) as used by Naqvi (1956) are as follows:

Molecular Formula: $(C_9H_{10})_n$

(n is the number of C_9H_{10} in one molecule)

Molecular Weight = $118.17 \times n$ gm/ gm-mole

Density (d_{ph}) = 1.05 gm/c.c.

Number of Molecules per c.c. (N_{ph}) = 5.35×10^{21} /c.c.

$$U_{ph} = \frac{9U_{CA} + 10U_{HA}}{9A_C + 10A_H}$$

where U_C and U_H are the mass absorption coefficients of carbon and of hydrogen for photons obtained from Siegbahn's book (1955). Using

$$T_{ph} = U_{ph} \times d_{ph}$$

we thus obtain Table 3 for photons interacting with the plastic shield.

Table 3

Photon Energy (Mev)	Mass Absorption Coeff.		Mean Free Path (cm)	Probability of Interaction in Plastic Phosphor	
	U_C (cm ² /gm)	U_H (cm ² /gm)		<u>1" Plate</u>	<u>5" Walls</u>
10	0.0195	0.0324	44.0	0.0559	0.250
20	0.0156	0.0214	59.1	0.0420	0.193
30	0.0147	0.0174	63.7	0.0390	0.181
40	0.0143	0.0154	66.1	0.0377	0.175
50	0.0142	0.0141	67.1	0.0372	0.173
60	0.0142	0.0132	67.4	0.0370	0.172
80	0.0143	0.0123	67.3	0.0370	0.172
100	0.0146	0.0118	66.6	0.0376	0.174

According to Hughes and Schwartz (1958), the neutron total cross section for carbon between 10 to 100 Mev appears to be about three times as big as its elastic cross section. However, no information about the elastic cross section for hydrogen is provided, nor is there any for its neighbouring elements. Assuming that for hydrogen half of the neutron total cross section is due to the elastic scattering process and that the

linear absorption coefficient is obtained by

$$T_{ph} = N_{ph} (2/3 \times 9S_C + 1/2 \times 10S_H)$$

we arrive at Table 4, applicable for neutrons interacting with the shield.

Table 4

<u>Neutron Energy</u> (Mev)	<u>Total Cross Sections</u>		<u>Mean Free Path</u> (cm)	<u>Probability of Interaction in Plastic Phosphor</u>	
	<u>S_C</u> (x 10 ²⁴ cm ²)	<u>S_H</u> (x 10 ²⁴ cm ²)		<u>1" Plate</u>	<u>5" Walls</u>
10	1.15	0.94	15.9	0.147	0.549
20	1.45	0.48	16.8	0.130	0.530
30	1.27	0.31	20.4	0.117	0.463
40	1.05	0.25	24.8	0.098	0.401
50	0.88	0.17	30.5	0.080	0.341
60	0.75	0.14	36.0	0.068	0.297
80	0.58	0.10	46.9	0.053	0.237
100	0.48	0.07	56.2	0.044	0.202

b. Function as Total Absorption Spectrometer for Neutral Component

When the NaI crystal is operated with the anticoincidence shield, almost all charged particles are eliminated without being recorded. As a charged particle passes through the shield, it suffers from ionization loss and thus initiates an a.c. pulse which will cancel the signal pulse produced in the interaction between the charged particle and the crystal.

Now, imagine that a neutral particle is incident on the shield; it either has an intact passage or interacts with the plastic phosphor. In the latter case, there are two possibilities. Either the secondary particles produced in the interaction are totally stopped in the plastic phosphor, thus eliminating the possibility of its being detected by the NaI crystal, or some of the secondary particles impinge on the crystal and hence initiate a pulse in the signal system; however, the secondary particles which are produced in the interaction between a neutral primary particle and the shield always contain at least one ionizing particle

(except the case of (n, γ) but this process is negligibly small for a neutron with energy greater than 10 Mev). This ionizing particle will generate an a.c. pulse in the anticoincidence system, thus cancelling the above mentioned signal pulse. Therefore, the probability for a neutral particle, interacting with the shield, to be recorded is negligibly small. In the former case, three possibilities must be considered. First, this neutral particle is not detected simply because of its missing the crystal or because of its penetrating through the crystal again without any interaction. Secondly, it interacts with the crystal but the secondary particles of the interaction are picked up by the shield; hence, it will not be recorded. Thirdly, both the primary neutral and its secondary particles are entirely stopped in the crystal, and this event is thus recorded in terms of its true energy and is said to be totally absorbed. With the anticoincidence shield in operation, the spectrometer records primarily only the totally absorbed neutral particles.

c. The Response of the Spectrometer to Neutral Particles

To study the response of the present spectrometer to a neutral particle, we have to examine (a) the probability of this incident neutral particle to pass through the shield and to interact with the NaI crystal, which is equal to its interaction probability with the crystal multiplied by its survival probability through the shield, and (b) the mean free path of this particle in the NaI crystal which gives some indication about the probability of the secondary particles (produced in the interaction between the primary neutral particle and the crystal) to be totally absorbed by the crystal. Hence, a good response of the spectrometer for a neutral particle is implied by a high probability for that particle to get through the shield and to interact with the crystal; further, the mean free path of such a particle should be much less than

the dimensions of the NaI crystal to ensure total absorption.

Using the Tables 1 to 4, the probabilities for a photon and for a neutron with a certain energy passing through the plastic phosphor and interacting with the crystal are calculated and the results are tabulated in Table 5 together with the ratio of the probability for a photon to that for a neutron.

Table 5

<u>Energy</u> (Mev)	<u>Prob. of Penetrating 1" Plate and Interacting in Crystal</u>			<u>Prob. of Penetrating 5" Walls and Interacting in Crystal</u>		
	<u>Photon</u>	<u>Neutron</u>	<u>Ratio</u>	<u>Photon</u>	<u>Neutron</u>	<u>Ratio</u>
10	0.84	0.47	1.8	0.67	0.25	2.7
20	0.90	0.47	1.9	0.76	0.26	3.0
30	0.92	0.48	1.9	0.78	0.29	2.7
40	0.93	0.49	1.9	0.80	0.33	2.4
50	0.94	0.50	1.9	0.80	0.36	2.2
60	0.94	0.51	1.9	0.81	0.39	2.1
80	0.94	0.52	1.8	0.81	0.42	2.0
100	0.95	0.52	1.8	0.81	0.44	1.9

By means of the Tables 1, 2, and 5 we can get some idea of the response of the spectrometer to photons and to neutrons. In Table 1, the mean free paths of the photon are much less than the assumed average possible path length (17.8 cm) in the crystal by a factor of two to four; therefore, it is quite reasonable to conclude that there is a relatively high probability of recording photons with an energy greater than 10 Mev. The situation is greatly different for neutrons. The mean free path for a neutron with an energy greater than 10 Mev is 22.6 cm which is greater than 17.8 cm; this implies a relatively high probability for the secondaries to be picked up by the shield even if the neutron interacts with the crystal, and thus a high probability for the failure of the spectrometer to record the neutron. Considering the ratios in Table 5 and the mean free paths, we conclude that the spectrometer has a much better

response to the cosmic photon than to the cosmic neutron. Such response functions could in principle be calculated but the task of doing so would be an enormous one.

d. Efficiency of Shield in Eliminating Charged Component

A differential spectrum obtained without anticoincidence and one with anticoincidence as shown in Figure 4 were utilized to estimate the efficiency of the anticoincidence system in the charged component cancellation. (a) Assume constancy in the intensities of cosmic radiation over the experimental time duration when the two spectra were obtained, and (b) assume no neutral particles in the cosmic radiation; therefore, the differential spectrum obtained without anticoincidence can be regarded as the spectrum of pure charged component and the differential spectrum obtained with anticoincidence as the spectrum of those charged particles which escape the anticoincidence cancellation. Then, we divided the two spectra into four energy loss ranges, and for each range we worked out the reduction of the charged component which is equal to the difference in the number of counts between the two spectra divided by that of the spectrum without anticoincidence. The results are given in Table 6.

Table 6

<u>Energy Loss Range</u> (Mev)	<u>Spectrum Without Anticoincidence</u> (cts/240 mins)	<u>Spectrum With Anticoincidence</u> (cts/240 mins)	<u>Reduction</u> (%)
11.5-48.8	77,294	24,908	67.8
48.8-126.3	88,863	3,828	95.7
126.3-199.6	28,039	404	98.6
<u>199.6-258.3</u>	<u>4,290</u>	<u>91</u>	<u>97.9</u>
11.5-258.3	198,260	29,229	85.3

However, the assumption (b) is subject to correction since the cosmic radiation does contain neutral particles. Hence, the difference in the

number of counts between the two spectra becomes larger as the spectrum with anticoincidence is essentially composed of totally absorbed neutral particle while the number of counts of the spectrum without anticoincidence becomes less; these two corrections combined together will enlarge the figures of the reduction listed in the Table 6. In general, the shield efficiency for eliminating the charged particles of energy loss greater than 50 Mev is at least 96%.

C. Determination of the Differential Spectrum

In all the experiments, a gamma ray of energy 1.12 Mev emitted from Zn^{65} served as a calibration source and the resolution of the spectrometer was found to be 16.8% at this low energy.

The experimental determination of a differential energy loss spectrum for the total cosmic radiation proceeded as follows. Firstly, to ensure an equal functioning of the three signal photomultipliers viewing the NaI crystal, their plate voltages were adjusted individually such that each of them, when operated alone, located the 1.12 Mev gamma ray at the same channel of the hundred channel kicksorter. For convenience, this gamma ray peak is called Zn peak. Secondly, together with a suitable choice in the output gains of the signal mixer and of the signal amplifier, the plate voltages of the three signal phototubes were further adjusted to obtain the energy range desired for the differential spectrum being investigated. On account of the fact that the hundred channel kicksorter accepted a ~~maximum~~ input pulse of 33 volts, a study in the high energy range required low plate voltages for the three phototubes, and low gains for the mixer and the amplifier; the reverse would lead to a low energy range. Through the calibration of the Zn peak position, the energy range of the cosmic ray spectrum was determined. Assuming that the energy E_x

required in the cosmic ray spectrum should appear in channel x with the mixer gain at b and the amplifier gain at a, and that the calibration spectrum of the Zn peak was to be done with the mixer gain at B and the amplifier gain at A, the Zn peak position must be located at channel y from the following formula,

$$y = x \frac{A}{a} \frac{B}{b} \frac{1.12}{E_x}$$

Hence, the plate voltages of the three phototubes were increased or decreased by an equal amount until the Zn peak was observed in channel y. Under the limitation of the present electronics, events with energy loss as high as 1 Bev could be studied. Thirdly, with the apparatus set for the desired energy range, a run was made by feeding the signal pulses into the kicksorter for a planned period of time, and the spectrum was subsequently printed out in terms of number of counts against each channel. Finally, the Zn peak position was calibrated again for any instability correction to the energy values of each channel in the spectrum.

For a neutral differential spectrum obtained with anticoincidence, the experimental procedure was exactly the same as mentioned above with the addition of the line-up of the eleven a.c. photomultipliers observing the shield and a stability check on the anticoincidence system. The plate voltages of the eleven phototubes were adjusted one by one with the Zn source nearby until each of the tubes gave approximately the same number of a.c. counts per unit time at the output of the gate pulse generator. As for the stability check, the a.c. pulses from the gate pulse generator were kept at a constant counting rate by adjusting the input bias voltage level so as to compensate for any slight shift of the electronics.

CHAPTER III
EXPERIMENTAL RESULTS

In this chapter results of experiments on the cosmic radiation energy loss spectra, on the nature of the neutral component and on the day-night effects on the cosmic radiation, together with the corresponding discussions and conclusions are presented.

In the present studies, corrections to the experimental data are essentially of two kinds; namely, the errors due to the drifts of the electronics and the meteorological effects on the intensity of cosmic radiation. To take care of these two factors and to obtain reasonable statistical accuracy, the time duration set for a run was compromised. The position of the Zn peak, which indicates any drift, was checked before and after a run, and the average was taken in the calculation of the energy range for the energy spectrum. Data for a run with a change in the Zn peak position greater than 4% was discarded. Temperature effects were neglected as it was reported by Bukata (1960) that the observed cosmic radiation intensity does not vary appreciably with temperature change. Corrections for atmospheric pressure variations were based on weather reports provided by the Department of Transport, Winnipeg, Canada and the barometric coefficients for the neutral component and for the total radiation which were determined by Bukata (1960) as $(0.579 \pm 0.160)\%$ per mb and $(0.239 \pm 0.028)\%$ per mb respectively.

To avoid the non-periodic solar activities which can have a drastic influence on the cosmic ray intensity, data utilized were checked with the Solar Geophysical data compiled monthly by U. S. Department of

Commerce etc., Boulder, Colorado, U. S. A. Data obtained during the occurrence of solar flares of importance 3 or greater were not used. Solar flares of importance less than 3 were neglected as they have not been reported as a significant cause of intensity changes.

A. Energy Spectra

By virtue of the characteristics of the present experimental arrangement, energy loss spectra can be determined only for the total cosmic radiation and for the neutral component. Unfortunately, the hundred channel kicksorter could not record the total radiation and its neutral component simultaneously, otherwise the charged component spectrum could be deduced directly from their difference. This section is devoted to the qualitative study of the energy spectra obtained by the present apparatus, and the purpose is threefold: to examine the general features of the differential spectra by means of a typical set of data, to make an estimate of the ratio of the neutral to the total radiation, and to compare the differential spectra obtained in two different years.

(i) Differential Energy Spectra

Figure 3 shows a typical sample of the differential energy loss spectra with energy up to 1075 Mev for the total radiation and the neutral components taken during 1960. The spectrum of the total radiation shows that the intensity decreases quite rapidly with increasing energy with a broad peak at about 90 Mev.

This peak in the total radiation spectrum is due to charged and neutral particles. It can be suppressed by the anticoincidence shield operated either without the six phototubes viewing the top plate or without the five viewing the bottom as shown by the curves of triangles and of crosses in Figure 3. This immediately suggests that most particles

producing the peak have an energy greater than the energy loss (because they interact with the bottom of the shield after passing through the crystal) and that they are charged particles. The possibility of their being protons is eliminated by Rossi's analysis (1948) that at sea level the proton content in the hard component is about 0.4% and the ratio of hard to soft components is about 2.5. Furthermore, no peak has been reported in the differential energy spectrum of the electron component for an energy greater than 40 Mev. On the other hand, Blackett (1937), Jones (1939), Hughes (1940) and Wilson (1946) and many others have shown that the hard component at sea level consists almost entirely of relativistic mu-mesons with a peak at about 750 Mev on their differential energy spectrum. Therefore, we confidently conclude that the peak in the present differential spectrum for the total radiation is mainly due to the contribution of the relativistic mu-mesons which lose about 90 Mev on their passage through the NaI crystal. For convenience, this peak is called the mu-peak subsequently.

Over the energy range from 750 to 1000 Mev, there appeared to be one or two small peaks in isolated runs; however, when a run of fifty six hours was made to check their definite existence, they were irreproducible and are therefore ascribed to the effects of statistical fluctuations.

Similarly, the differential spectral curves of the neutral component have a common shape: the intensity falls very rapidly with increasing energy and reduces practically to zero beyond 430 Mev. The failure of the spectrometer to record the neutral particles of energy greater than about 430 Mev is due to the fact that the present NaI crystal is not large enough to contain all the shower particles generated in the crystal by such particles (see Kantz and Hofstadter(1953, 1954)), and any energy leakage initiates the anticoincidence shield which produces cancellation.

Log-log plots were tried for the spectra of the total radiation

and of the neutral component but they showed nothing significant.

(ii) Relative Intensities of the Neutral to the Total Radiation

By removal of the anticoincidence pulses from some or all of the eleven photomultipliers viewing the plastic shield, four spectra as illustrated in Figure 4 were obtained in four consecutive runs for the purpose of estimating the ratio of the detected neutral component to the detected total radiation, and the ratio of the totally absorbed neutral to the totally absorbed total radiation.

a. Ratio of Detected Neutral to Detected Total Radiation

The spectrum of the detected total radiation was determined without anticoincidence. To obtain the spectrum of the detected neutral component, the five phototubes observing the bottom of the shield were disconnected from the a.c. mixer; hence, nearly all charged particles are eliminated except an unknown but small portion from the sides and the bottom of the shield whose interaction with the phosphor is not detected by the six phototubes around the top plate. As a result, the recorded number of counts sets an upper limit to the detected neutral particles.

For each of these two spectra, the number of counts was summed up from channel number 4 to 90. On account of the relatively small number of counts beyond channel number 90 (less than 1%), the integrated number can be regarded as the number of particles with an energy loss greater than 11.5 Mev. The result is presented in Table 7.

Table 7

<u>Detected Total Radiation</u> (cts/240 mins)	<u>Detected Neutral Particles</u> (cts/240 mins)	<u>Ratio</u> (%)
198,260	35,337	17.8

b. Ratio of Totally Absorbed Neutral to Totally Absorbed Cosmic Radiation

With the six photomultipliers around the top plate removed from the anticoincidence system, the spectrum represents the totally absorbed charged and neutral particles. Since there is an unknown amount of charged particles from the sides of the shield which are totally absorbed but eliminated by the five phototubes at the bottom of the shield, the recorded number of counts can be taken as a lower limit for the totally absorbed radiation. The totally absorbed neutral spectrum was obtained with all the eleven phototubes viewing the shield. Table 8 gives the ratios for various energy ranges.

Table 8

<u>Energy Range</u> (Mev)	<u>Totally Absorbed Cosmic Particles</u> (cts/ 240 mins)	<u>Totally Absorbed Neutral Particles</u> (cts/ 240 mins)	<u>Ratio</u> (%)
11.5- 48.8	31,465	24,906	81.4
48.8-126.3	7,048	3,828	54.3
126.3-199.6	1,183	404	34.2
<u>199.6-258.3</u>	<u>276</u>	<u>91</u>	<u>33.0</u>
11.5-258.3	39,972	29,229	73.1

From Tables 7 and 8, some remarks on the nature of cosmic radiation near sea level observed with the present apparatus can be made:

(1) Over 82% of the cosmic radiation with energy loss greater than 11.5 Mev in the NaI crystal are charged and they pass through the top of the shield. (see Table 7)

(2) The difference between the number of the detected neutral and that of the totally absorbed neutral will include those charged which are not eliminated by the six phototubes around the top of the shield and those neutrals which are not totally absorbed by the crystal. If we assume zero contribution of the latter, then about 3% (as an upper limit)

of the total radiation are charged particles with an energy loss greater than 11.5 Mev which are not eliminated by the six phototubes around the top plate of the shield. (deduced from Tables 7 and 8)

(3) For the energy loss range between 11.5 and 258.3 Mev, 93.4% of the detected charged component pass through the crystal while 82.9% of the detected neutral are totally absorbed by the crystal. (deduced from Tables 7 and 8)

(4) So far as totally absorbed particles are concerned neutral particles are dominant in the low energy range from 11.5 to 126.3 Mev, and in general as the energy increases the content of the neutral decreases more rapidly as compared with the charged component. In high energy ranges charged particles become the majority. (see Table 8)

(iii) Comparison of Energy Spectra Observed in 1960 and 1961

In Figure 5, two typical differential spectra of the total radiation (one taken in 1960 and the other in 1961) were compared. The mu-peak in 1961 appeared sharper than that in 1960, and the position of the former was located at 92.1 ± 0.5 Mev while the latter at 91.8 ± 0.5 Mev. The change in counting rates for the cosmic ray particles with energy loss greater than 11.5 Mev (neglecting the small number of particles beyond energy 285.3 Mev which is less than 1%) is given in Table 9, using the value of 1960 as 100%.

Table 9

<u>Counting Rate</u> 1960	(cts/240 mins) 1961	<u>Ratio</u> (%)
198,260	230,785	116.4

For the two neutral differential spectra of 1960 and 1961 as plotted in Figure 5, the variation in counting rates over corresponding

energy ranges is tabulated in Table 10.

Table 10

<u>Energy Range</u> (Mev)	<u>Counting Rate</u> (cts/240 mins)		<u>Ratio</u> (%)
	1960	1961	
11.5- 48.8	24,906	25,926	104.1
48.8-126.3	3,828	3,371	88.1
126.3-199.6	404	286	70.1
<u>199.6-258.3</u>	<u>91</u>	<u>48</u>	<u>53.0</u>
11.5-258.3	29,229	29,631	101.4

Results of the comparison are stated as follows:

- (1) The mu-peak position can be regarded as constant.
- (2) For all cosmic radiation with energy loss greater than 11.5 Mev, the total radiation increases by 16.4% while the neutral increases by 1.4%. This indicates that the charged component has a much bigger change than the neutral.
- (3) Within the energy range 11.5-258.3 Mev, the number of low energy neutrals increases while neutrals with energy greater than 48.8 Mev decrease sharply in number with energy. The small change in number for the whole range may indicate some fluctuation in the energy distribution among a practically constant number of neutral particles, or some sort of mechanism regulating the energy distribution. The real existence of this phenomenon requires further confirmation from more experiments.

B. Nature of the Neutral Component as Detected by the Spectrometer

For the purpose of experimentally investigating the nature of the neutral cosmic particles detected by the present apparatus, a lead absorption experiment was done to determine the absorption curve of the neutral component.

Experimentally, a frame of steel angle-bars was built to hold

a large weight of lead. The mass and the thickness of the steel bars were kept to a minimum, so that the effect of the interaction between the cosmic radiation and the steel is negligibly small. Twenty pieces of lead sheet, each of dimensions of 2'x 2'x 1/16", and twenty five lead blocks each 4"x 4"x 2" were used as absorbers in different thickness combinations. They were placed above and close to the top of the anticoincidence shield, thus reducing the transition effect in the air between the lead and the detector. Experimental data were collected in terms of differential spectra of the neutral component, and so there was nothing new in the experimental procedure. Four energy ranges were selected to cover the whole spectrum. At lower energies, the energy ranges were made narrow because counting rates here are relatively high and comparison with the theoretical absorption coefficients (which vary more rapidly at low energies) is therefore easier. The experimental results are tabulated in Table 11 and plotted in Figure 6.

Table 11

<u>Lead Thickness</u> (10 ⁻³ in.)	<u>Counting Rate (cts/840 mins)</u>			
	<u>10-12 Mev</u>	<u>20-24 Mev</u>	<u>40-60 Mev</u>	<u>100-270 Mev</u>
0.0	27,940	16,226	11,506	2,363
70.8	25,848	15,196	10,512	2,263
217.3	22,249	12,364	8,297	1,748
624.9	15,511	6,857	4,232	993
1095.0	10,274	4,868	3,087	833
1370.9	8,745	4,152	2,793	762
2419.9	6,741	3,335	2,526	719
2898.1	6,158	3,266	2,525	749
3370.9	5,929	3,129	2,326	732

On a semi-log plot with counting rate as the ordinate and lead thickness as the abscissa, the four absorption curves appeared to have common qualitative features: the intensity decreases with increasing thickness

and tends to reach a constant value at large absorber thicknesses.

The analysis of each of these experimental curves was as follows and is illustrated in Figure 7 for the one of 10-12 Mev. First, the constant value of the intensity at large thicknesses was drawn as a horizontal line designated as the background intensity. The relative background is defined as the ratio of the background intensity to the intensity of the neutral component at zero lead thickness. Then, on semi-log paper a curve was constructed by subtracting the background intensity from the original experimental curve. This curve appears to be approximately a straight line (for all four sets of data). This implies that the neutral component detected is essentially composed of a single kind of particle. However, the presence of a small amount of other kind of particles can not be excluded. Since the incident neutrals have a directional distribution and hence the traversed path length of individual particle in the absorber depends on its incident zenith angle, the determined slope of the straight line (called observed linear absorption coefficient) is in fact a product of the linear absorption coefficient of the incident particles for lead and the coefficient of the statistical weighted average path (shortened as effective path coefficient) of these particles in the absorber. As the experiments were done near the sea level, there are two significant hypotheses on the kind of cosmic particle accounting for this straight line; namely, either photons or neutrons. The effective path coefficients for photons and for neutrons were evaluated individually by comparing the observed linear absorption coefficient with their absorption coefficients for lead (these values were adopted from Siegbahn's book (1955) for photons and from Hughes and Schwartz (1958) for neutrons). The corresponding zenith angle of the average incident direction was thus deduced by taking the anti-cosine of the reciprocal

of the effective path coefficient. Table 12 gives the results of the analysis.

Table 12

	<u>Energy Range (Mev)</u>			
	<u>10-12</u>	<u>20-24</u>	<u>40-60</u>	<u>100-270</u>
Background (cts/340 mins) :	5,900	3,200	2,400	730
Relative Background (%) :	21.1	19.7	20.9	30.9
Observed Abs. Coeff. (cm^{-1}) :	0.587	0.748	0.986	1.191
<u>Photon Hypothesis</u>				
Abs. Coeff. (cm^{-1}) :	0.580	0.725	0.925	1.148
Eff. Path Coeff. :	1.013	1.032	1.065	1.045
Zenith Angle (degree) :	9.1	14.3	20.1	16.8
<u>Neutron Hypothesis</u>				
Abs. Coeff. (cm^{-1}) :	0.161	0.189	0.145	0.148
Eff. Path Coeff. :	3.65	3.96	6.79	8.05
Zenith Angle (degree) :	74.1	75.4	81.5	82.9

From the above results, it can be seen that photons give consistent values for the effective path coefficients of the four energy ranges and more reasonable zenith angles. Therefore, the four straight lines are concluded to be the absorption curves of photons primarily.

To assess the amount of neutrons possibly detected in the neutral component for a certain energy range, 2% of the counting rate without background at zero lead thickness was assumed as a neutron contribution. A theoretical absorption curve for this 2% neutron component was deduced by using the linear absorption coefficient for neutrons and a path coefficient equal to that of the photon pertinent to the desired energy range. The other 98% was then assigned to be the photon intensity, and its theoretical absorption curve was also obtained in like manner. These two theoretical absorption curves and the background horizontal line were combined to form a new curve which was utilized for comparison with the original experimental curve. Such combined curves were also made for assumptions of 5% and 10% neutrons. In general, for all four energy ranges

the curves of 5% and 10% neutrons agree badly with the experimental curve while the zero % neutron curve gives the best fit and the 2% neutron curve is the second best except in one case. For the 100-270 Mev range the 2% neutron curve gives a better fit with the experimental curve than the zero % one.

The background intensity is that of the neutral particles coming in from the sideward directions which are not blocked by the lead lying on the top of the shield; as a consequence, it is not affected by a change of the lead thickness. The relative background discloses the portion of the neutrals passing through the shield walls, which amounts to about one-fifth of the total neutral component for the three low energy ranges. For the 100-270 Mev range it has a higher value than the others by one-third.

As far as the neutron content in the neutral component is concerned, the result of the foregoing analysis is by no means conclusive. Experimentally, it is difficult to determine accurately the background intensity which is the key to the whole analysis. An overestimate of this background will mask the existence of the neutron component because neutrons have much lower value for their lead absorption coefficient as compared with that of photons and their intensity is low as compared with the background. The situation could be greatly improved by doing a much more elaborate absorption experiment using a much thicker absorbers. Ideally, one would like to have the shield completely surrounded with lead absorber but this poses practical difficulties.

In conclusion, while these lead absorption experiments do not conclusively establish the exact nature of the detected neutrals, the analysis presented does show that the assumption of greater than or equal to 98% photon and less than or equal to 2% neutron is quite consistent with the

experimental observation; furthermore it is roughly what one might expect from the work of others on the general nature of the cosmic radiation at sea level.

C. Day-Night Variation of Cosmic Radiation

As the sun has been regarded for a long time as a possible source of some of the cosmic radiation, a study on the day-night variations of cosmic radiation during periods of no intensive solar activity may help to reveal to what extent the normal sun is such a source. Though the radiation observed near sea level is secondary in nature, its variation has a direct bearing on the primary radiation at the top of the atmosphere.

Experiments were conducted to investigate the day-night difference in the intensities of the mu-peak region in the total radiation differential spectrum and of the neutral component. Differential spectra were taken twice a day; six hours before the local noon time and six hours after constituted the time duration for the day run while the other twelve hours constituted the night run. The experimental procedure in obtaining the differential spectra was exactly the same as described in Chapter II. The analysis on each set of data was performed by summing up the number of counts over the energy range of interest and by calculating the difference between the counts of the day run and that of the night run. While the day-night difference serves as evidence for a day-night effect, the relative day-night difference, which is defined as the day-night difference divided by the number of counts of the day run, indicates the importance of any solar contribution.

(i) The Mu-Peak Region

The mu-peak region is defined as the energy loss range from 48.8 to 126.3 Mev in the total radiation differential spectrum. Eighteen

sets of data are given in Table 13 accompanied with the corresponding analysis.

Table 13

The Mu-Peak Region : 48.8-126.3 Mev

Date	Experimental Data		Analysis Results	
	Night (cts/700 mins)	Day (cts/700 mins)	Day-Night Diff. (cts/700 mins)	Rel. Day-Night Diff. (%)
1960				
Aug. 12-13	310,108±557	313,054±560	+2,946±1,117	+0.94±0.36
Aug. 18-19	299,718±547	307,890±555	+8,172±1,102	+2.65±0.36
Aug. 19-20	303,092±550	304,142±551	+1,050±1,101	+0.35±0.37
Aug. 20-21	306,182±554	296,646±546	-9,536±1,100	-3.21±0.37
Aug. 21-22	297,185±545	293,782±541	-3,403±1,086	-1.16±0.37
Aug. 22-23	300,921±549	303,763±550	+2,842±1,099	+0.94±0.36
Aug. 23-24	305,965±554	305,929±554	-36±1,108	-0.01±0.36
Aug. 24-25	306,498±555	298,614±546	-7,884±1,101	-2.64±0.37
Aug. 25-26	308,891±556	311,372±558	+2,481±1,114	+0.80±0.36
Aug. 26-27	310,614±557	305,484±553	-5,130±1,110	-1.68±0.36
Aug. 28-29	304,246±551	299,170±547	-5,076±1,098	-1.70±0.37
Aug. 29-30	294,721±543	303,925±550	+9,204±1,093	+3.03±0.36
Aug. 30-31	304,463±551	299,700±547	-4,763±1,098	-1.59±0.37
Aug. 31-Sep.1	302,086±550	287,287±536	-14,799±1,086	-5.15±0.38
Sep. 4 - 5	305,063±553	304,396±552	-667±1,105	-0.22±0.36
Sep. 13-14	312,343±559	313,179±560	+836±1,119	+0.27±0.36
Sep. 17-18	315,196±561	312,347±559	-2,849±1,120	-0.91±0.36
Sep. 29-30	319,078±565	320,680±566	+1,602±1,131	+0.50±0.35
<hr/>				
Aug. 12- Sep. 30	5,506,370 ±9,957	5,481,360 ±9,931	-25,010 ±19,889	-0.46 ±0.37

In total, the day-night difference is negative and its absolute value is comparable with its standard error. Coupled with a very small relative day-night difference, it can be concluded that a day-night effect is very small if it exists at all. The maximum possible value for the relative day-night difference from this experiment is less than or equal to 0.82%.

(ii) Neutral Component

To study the day-night effect on the totally absorbed neutral particles, the whole differential energy spectrum was arbitrarily divided into four energy ranges. Ten sets of data were collected for analysis

and the results are shown in Tables 14 to 17.

Table 14

Neutral Component: 11.5-48.8 Mev

Date	Experimental Data		Analysis Results	
	Night (cts/700 mins)	Day (cts/700 mins)	Day-Night Diff. (cts/700 mins)	Rel. Day-Night Diff. (%)
1960				
Jul. 18-19	68,483±262	69,273±264	+790±526	+1.14±0.76
Jul. 20-21	70,987±266	70,663±266	-324±532	-0.46±0.76
Jul. 21-22	70,987±266	70,678±266	-309±532	-0.44±0.76
Jul. 22-23	69,813±264	68,202±261	-1,611±525	-2.36±0.77
Jul. 23-24	69,332±264	71,375±267	+2,043±531	+2.86±0.74
Jul. 25-26	70,401±266	70,092±265	-309±531	-0.44±0.76
Jul. 27-28	69,734±264	68,066±261	-1,668±525	-2.45±0.77
Jul. 29-30	73,148±270	70,926±266	-2,222±536	-3.13±0.75
Jul. 30-31	72,222±269	73,179±270	+957±539	+1.31±0.74
Jul. 31-Aug. 1	71,073±267	72,283±269	+1,210±536	+1.67±0.74
<hr/>				
Jul. 18- Aug. 1	706,180 ±2,658	704,737 ±2,655	-1,443 ±5,313	-0.20 ±0.74

Table 15

Neutral Component: 48.8-126.3 Mev

Date	Experimental Data		Analysis Results	
	Night (cts/700 mins)	Day (cts/700 mins)	Day-Night Diff. (cts/700 mins)	Rel. Day-Night Diff. (%)
1960				
Jul. 18-19	8,696±93	8,508±92	-188±185	-2.21±2.17
Jul. 20-21	9,190±96	8,778±94	-412±190	-4.69±2.16
Jul. 21-22	9,025±95	9,101±95	+76±190	+0.84±2.10
Jul. 22-23	8,794±94	8,706±93	-88±187	-1.01±2.15
Jul. 23-24	8,835±94	9,689±98	+854±192	+8.81±1.98
Jul. 25-26	9,279±96	8,969±95	-310±191	-3.46±2.13
Jul. 27-28	8,682±93	8,962±95	+280±188	+3.12±2.09
Jul. 29-30	10,064±100	9,223±96	-841±196	-9.12±2.12
Jul. 30-31	9,833±99	9,588±98	-245±197	-2.56±2.06
Jul. 31-Aug. 1	9,351±97	9,405±97	+54±194	+0.57±2.05
<hr/>				
Jul. 18- Aug. 1	91,749±957	90,929±953	-820±1,910	-0.90±2.10

Table 16

Neutral Component: 126.3-199.6 Mev

Date	Experimental Data		Analysis Results	
	Night (cts/700 mins)	Day (cts/700 mins)	Day-Night Diff. (cts/700 mins)	Rel. Day-Night Diff. (%)
1960				
Jul. 18-19	623±25	683±26	+60±51	+8.78±7.46
Jul. 20-21	749±27	659±26	-90±53	-13.66±8.05
Jul. 21-22	738±27	669±26	-69±53	-10.31±7.92
Jul. 22-23	676±26	677±26	+1±52	+0.15±7.80
Jul. 23-24	687±26	819±29	+132±55	+16.12±6.72
Jul. 25-26	702±26	751±27	+49±53	+6.52±7.05
Jul. 27-28	686±26	778±28	+92±54	+11.83±6.94
Jul. 29-30	840±29	742±27	-98±56	-13.21±7.54
Jul. 30-31	780±28	777±28	-3±56	-0.39±7.28
Jul. 31-Aug. 1	738±27	783±28	+45±55	+5.75±7.03
<hr/>				
Jul. 18-Aug. 1	7,219±267	7,337±271	+119±538	+1.61±7.34

Table 17

Neutral Component: 199.6-258.3 Mev

Date	Experimental Data		Analysis Results	
	Night (cts/700 mins)	Day (cts/700 mins)	Day-Night Diff. (cts/700 mins)	Rel. Day-Night Diff. (%)
1960				
Jul. 18-19	124±11	109±10	-15±21	-13.76±19.26
Jul. 20-21	107±10	86±9	-21±19	-24.42±22.10
Jul. 21-22	155±12	139±12	-16±24	-11.51±17.27
Jul. 22-23	122±11	124±11	+2±22	+1.61±17.71
Jul. 23-24	116±11	130±11	+14±22	+10.77±16.92
Jul. 25-26	117±11	146±12	+29±23	+19.86±15.75
Jul. 27-28	123±11	145±12	+22±23	+15.17±15.85
Jul. 29-30	131±11	98±10	-33±21	-33.67±21.41
Jul. 30-31	147±12	115±10	-32±22	-27.83±19.15
Jul. 31-Aug. 1	138±12	110±10	-28±22	-25.45±20.00
<hr/>				
Jul. 18-Aug. 1	1,280±112	1,202±107	-78±219	-6.49±18.22

For each of the four energy ranges, the results lead to a conclusion similar to that for the mu-peak region of the total cosmic radiation. Three ranges

show a negative day-night difference while one is positive but with a probable error three times as big as itself. As a matter of fact, the standard errors of the day-night difference for all four ranges are greater than differences themselves.

When 11.5-258.3 Mev is taken as a whole range as shown in Table 18, the day-night difference is negative; and the relative difference is again very small (about 0.3%). The maximum possible value for the relative difference is less than 1%.

Table 18

Neutral Component: 11.5-258.3 Mev

Date	Experimental Data		Analysis Results	
	Night (cts/700 mins)	Day (cts/700 mins)	Day-Night Diff. (cts/700 mins)	Rel. Day-Night Diff. (%)
1960				
Jul. 18-19	77,926 \pm 279	78,573 \pm 280	+647 \pm 559	+0.82 \pm 0.86
Jul. 20-21	81,033 \pm 285	80,186 \pm 283	-847 \pm 568	-1.06 \pm 0.71
Jul. 21-22	80,905 \pm 284	80,587 \pm 284	-318 \pm 568	-0.39 \pm 0.70
Jul. 22-23	79,405 \pm 282	77,708 \pm 278	-1,697 \pm 560	-2.18 \pm 0.72
Jul. 23-24	78,970 \pm 281	82,013 \pm 286	+3,043 \pm 567	+3.71 \pm 0.70
Jul. 25-26	80,499 \pm 284	79,958 \pm 282	-541 \pm 566	-0.68 \pm 0.71
Jul. 27-28	79,225 \pm 282	77,951 \pm 279	-1,274 \pm 561	-1.63 \pm 0.72
Jul. 29-30	84,183 \pm 290	80,989 \pm 284	-3,194 \pm 574	-3.94 \pm 0.71
Jul. 30-31	82,982 \pm 288	83,659 \pm 289	+677 \pm 577	+0.81 \pm 0.69
Jul. 31-Aug. 1	81,300 \pm 285	82,581 \pm 287	+1,281 \pm 572	+1.55 \pm 0.70
<hr/>				
Jul. 18- Aug. 1	806,428 \pm 2,840	804,205 \pm 2,832	-2,223 \pm 5,672	-0.28 \pm 0.72

In conclusion, the experimental results for the mu-peak region of the total spectrum (mostly mu-mesons) and the neutral component do not give definite evidence of a day-night effect.

However, the occasional occurrence of a large day-night difference is of interest, for example Aug. 31-Sep. 1 when the relative day-night difference was (-5.15 \pm 0.38)%. This kind of occurrence may be due to an unseen solar flare on the hidden side of the sun as suggested by



Carmichael and Steljes (1961), and Covington and Harvey (1961).

Further work along these lines is thought to be desirable, particularly if data could be collected simultaneously for both the total and the neutral spectra. This will be feasible when a 400 channel pulse height analyser, now on order, is received.

D. A Sudden Increase in the Photon Component of Cosmic Radiation

During the course of these studies, on May 4, 1960 it was observed that the intensity of both the charged and neutral components increased suddenly at 10:45 \pm 15 minutes G.M.T. These increases are definitely related to the occurrence of a solar flare which started at 10:20 and ended at 10:25 G.M.T. of the same day (see Rose (1960)).

The experimental arrangement was essentially the same as that stated in Chapter II except that instead of the hundred channel kicksorter, two integral pulse height analysers were used with settings at 12 and 35 Mev to record simultaneously the neutral component and the total radiation. Counts were registered by four glow transfer scalers which were photographed every 15 minutes.

Preliminary study of this extraordinary event has been made on the neutral component (designated as P) and the charged component (designated as C) for various energy ranges as shown in Figure 8. The counting rate is plotted as a percentage of the mean counting rate over the period from 05:00 to 13:00 hours and in each case the horizontal dashed lines represent the limits of the probable counting error. As the pressure remained fairly constant over this period, no corrections have been made for pressure variations. These results may be summarized as follows:

(1) The increase in counting rate for the C component (essentially mu-mesons) is 10-15% above the mean in agreement with data obtained using

meson telescopes (Rose, 1960).

(2) The increase for the P component (essentially gamma-rays) with events above 35 Mev (about 50-60%) is considerably greater than the increase for those from 12-35 Mev (about 10-15%).

An interpretation of this result cannot be given at the present time, and the above observations have already been reported by Standil, Bukata and Chin (1960).

E. Conclusions

In spite of the insufficient knowledge about its response function, the present spectrometer can be used with reasonable counting rates and therefore tolerable statistics to study the time variation of the photon component up to a few hundred Mev. This has not been investigated by the other workers. With the arrival of the recently ordered 400 channel pulse height analyser, more refined experiments can be done on both day-night effects and solar flare effects. With this analyser all the information that the present spectrometer can provide (for both the charged and the neutral components) can be simultaneously recorded and tabulated. This recording and tabulating will be done on a continuous basis with the data punched out at pre-determined and equal time intervals of the order of 15 minutes. Any time variations in either one or both components and in any energy range will thus be studied with a reasonable time resolution.

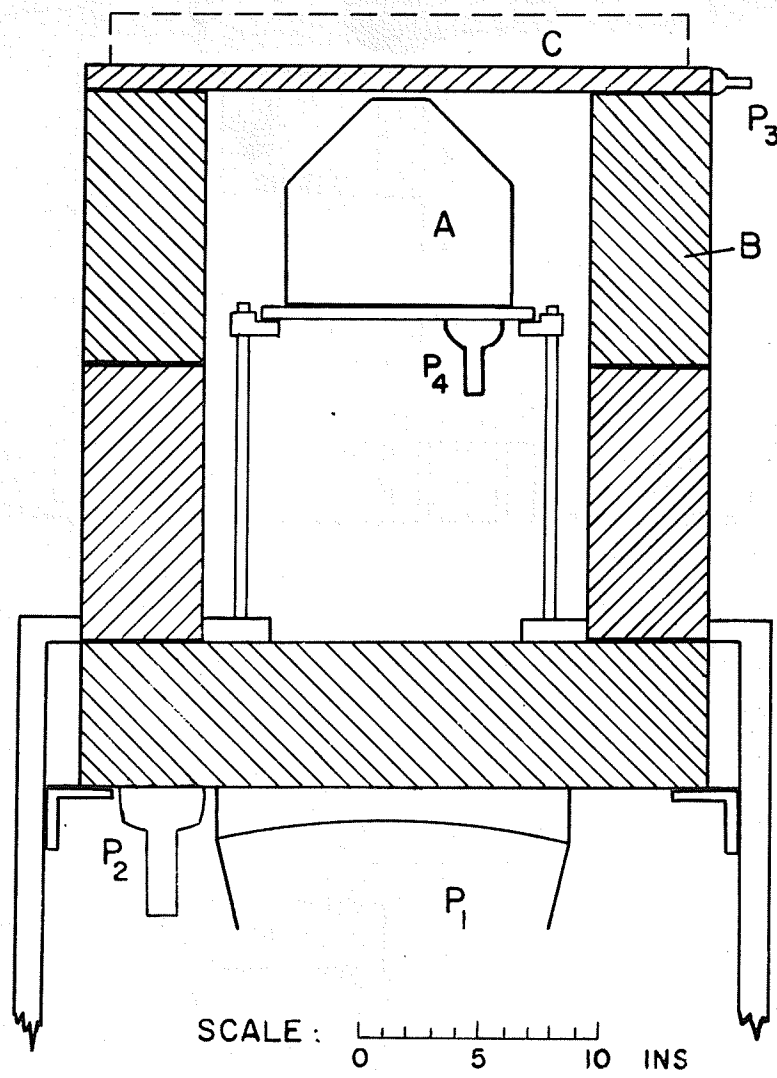
R E F E R E N C E S

- Blackett, P.M.S., 1937, Proc. Roy. Soc. A 159, 1.
- Bukata, R.P., 1958, Summer Thesis, University of Manitoba.
- Bukata, R.P., 1960, Master's Thesis, University of Manitoba.
- Carmichael, H. and J.F. Steljes, 1961, Phys. Rev. Letters, 6, 49.
- Cernigoi, G. and G. Poiani, 1954, Nuovo Cim., 11, 41.
- Chou, C.N., 1953, Phys. Rev., 90, 473.
- Clay, J. and E. van Alphen, 1951, Physica, 17, 711.
- Covington, A.E. and G.A. Harvey, 1961, Phys. Rev. Letters, 6, 51.
- Harshaw Chemical Company, 1960, Harshaw Scintillation Phosphors,
(Cleveland, Ohio, U.S.A.), p. 10.
- Hughes, D.J., 1940, Phys. Rev., 57, 592.
- Hughes, D.J. and R.B. Schwartz, 1958, Neutron Cross Sections, Brookhaven,
National Report BNL-325, 2nd edition, (U.S. Government
Printing Office, Washington, D. C.), pp. 74, 97, 113, 234, 306.
- Janossy, L. and B. Rossi, 1940, Proc. Roy. Soc., A 175, 88.
- Jones, H., 1939, Rev. Mod. Phys., 11, 235.
- Kameda, T., 1960, J. Phys. Soc. Japan, 15, 1175.
- Kantz, A. and R. Hofstadter, 1953, Phys. Rev., 89, 607.
- Kantz, A. and R. Hofstadter, 1954, Nucleonics, 12, 36.
- Loveridge, W.D., 1959, Master's Thesis, University of Manitoba.
- Naqvi, S.I.H., 1956, Master's Thesis, University of Manitoba.
- Rose, D.C., 1960, Can. J. Phys., 38, 1224.
- Rossi, B., 1948, Rev. Mod. Phys., 20, 537.
- Siegbahn, K., 1955, Beta- and Gamma-Ray Spectroscopy, (Amsterdam; North-
Holland Publishing Co.), App. I, pp. 859, 860, 873.

Standil, S. and W.D. Loveridge, 1959, Rev. Sci. Instr. 30, 931.

Standil, S., R.P. Bukata and F.K. Chin, 1960, Can. J. Phys., 39, 229.

Wilson, J.G., 1946, Nature, 158, 415.



- A NaI (TI) CRYSTAL
- B PLASTIC PHOSPHOR ANTICOINCIDENCE SHIELD
- C Pb USED ONLY IN LEAD ABSORPTION EXPERIMENT
- P₁ DU MONT K1328 PHOTOMULTIPLIER
- P₂ ONE OF FOUR DU MONT 6364 PHOTOMULTIPLIERS
- P₃ ONE OF SIX DU MONT 6292 PHOTOMULTIPLIERS
- P₄ ONE OF THREE DU MONT 6364 PHOTOMULTIPLIERS

FIG. 1 TOTAL ABSORPTION SPECTROMETER

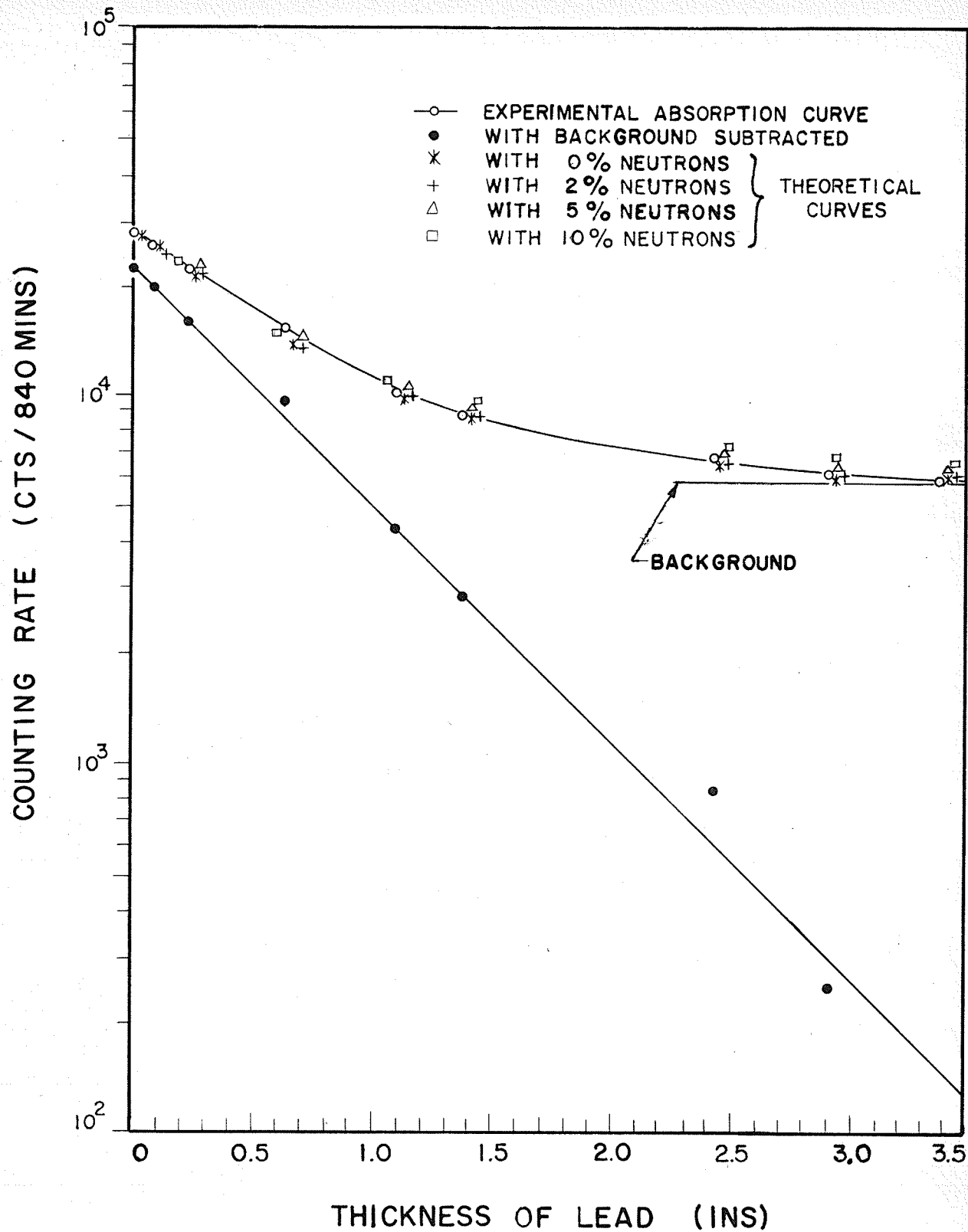


FIG. 7 ANALYSIS ON THE EXPERIMENTAL
 ABSORPTION CURVE OF NEUTRAL
 COMPONENT FOR ENERGY 10-12 MEV

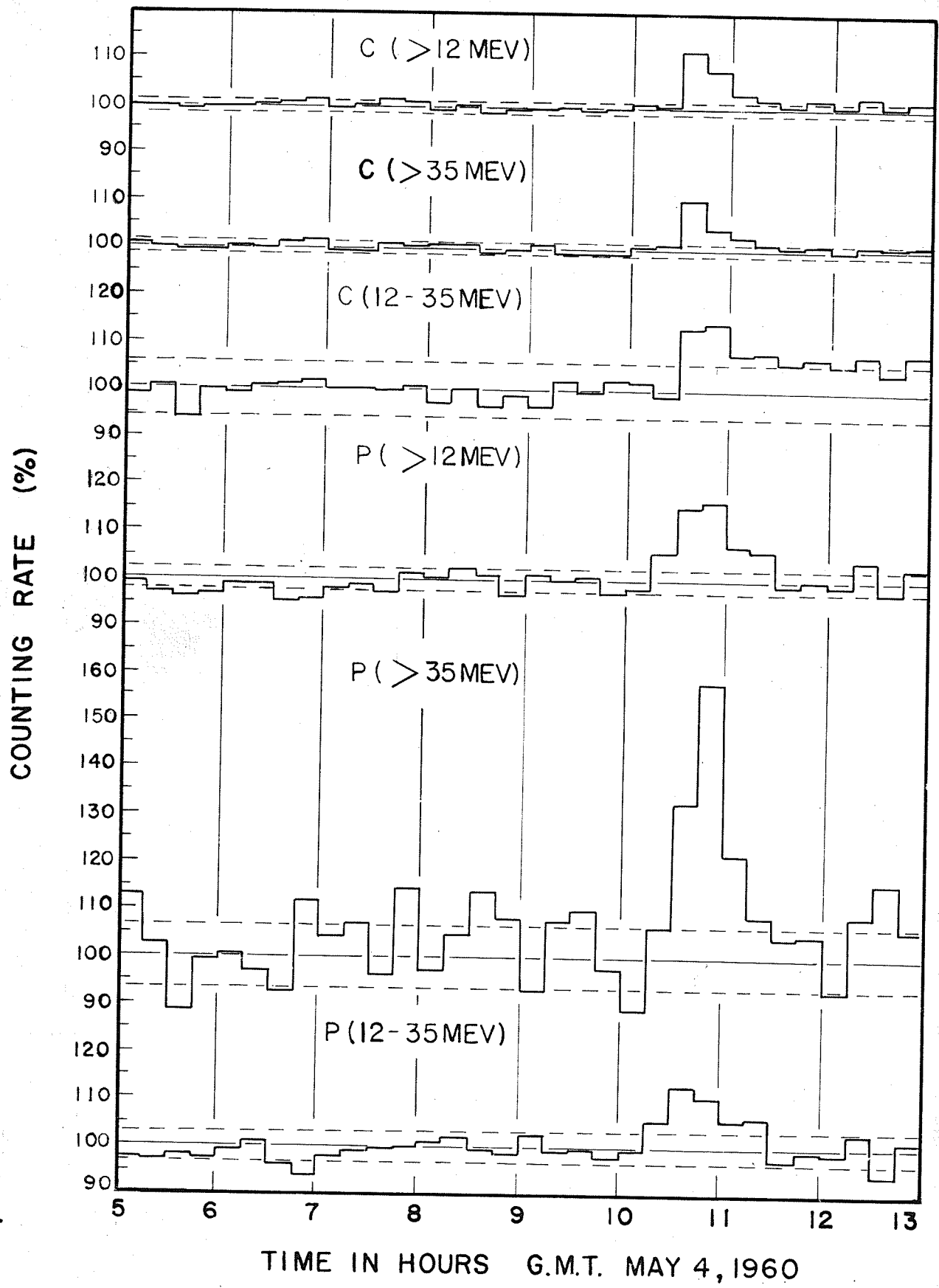


FIG. 8 THE EVENT OF MAY 4, 1960